

Thermal, Electrical and Magnetic Properties of the Ferromagnetic Dense Kondo System CeSi_x

Nobuya SATO, Hiroshi MORI, Takeo SATOH,
Tsuneo MIURA[†] and Humihiko TAKEI[†]

*Department of Physics, Faculty of Science,
Tohoku University, Sendai 980*

*[†]Institute for Iron, Steel and Other Metals,
Tohoku University, Sendai 980*

(Received July 9, 1987)

Single crystals of the ferromagnetic dense Kondo system CeSi_x were grown, and the specific heat, the electrical resistivity and the magnetic susceptibility were measured. Electrical resistivity measurements clearly show the typical Kondo behavior, which unambiguously tells that CeSi_x is a ferromagnetic dense Kondo system. The appreciable anisotropy of the magnetic susceptibility is analyzed with the crystalline field effect and a conjecture is made that the ground doublet is a Γ_7 -like doublet.

§1. Introduction

CeSi_2 is a member of $\alpha\text{-ThSi}_2$ type intermetallic compound, as shown in Fig. 1. This structure is known to be found only for silicides and germanides. It was found that CeSi_2 exhibits various anomalies associated with the intermediate valence or the Kondo effect of Ce ions.¹⁾ The investigation was extended to the Si-deficient system, CeSi_x , which retains the same $\alpha\text{-ThSi}_2$ type structure down to about $x=1.55$.²⁾ Measurements of the magnetic susceptibility and the specific heat revealed that in the composition range $1.83 < x \leq 2.00$ the system is nonmagnetic at low temperatures and for $x \leq 1.83$ the system undergoes a sharp ferromagnetic transition which is indicated by the divergence of the susceptibility around 10 K.^{2,3)} The magnetization measurements revealed that the magnetic moment per Ce atom in the ordered state is much reduced and it becomes almost zero near the critical Si-concentration ($x=1.83$).^{3,4)} Further, the electronic specific heat coefficient, γ , increases very rapidly when the Si concentration approaches the critical value $x_c \approx 1.83$, either from the nonmagnetic region or from the magnetic region.⁵⁾ Such a trend is very similar to the theoretical prediction obtained for an itinerant electron system near a ferromagnetic instability.^{6,7)} In these respects, the

magnetically ordered CeSi_x system can be regarded as a kind of weak ferromagnetic system. Magnetic entropy below T_c , S_m , is much smaller than $R \ln 2$, where R is the gas constant.²⁾

On the basis of these various experimental results, it was considered that the CeSi_x system is the first example of a dense Kondo system in which the ferromagnetic correlation is dominant. This point is very remarkable compared with widely studied many dense Kondo

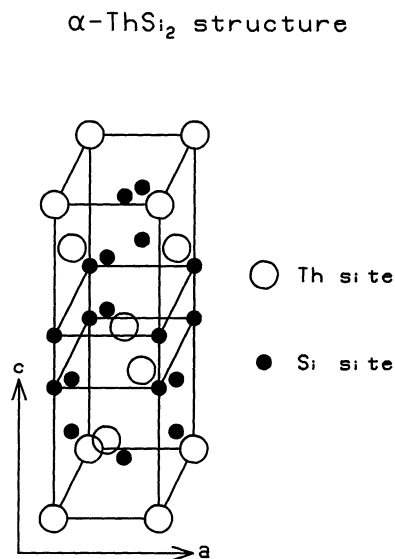


Fig. 1. Crystal structure of CeSi_2 .

systems where the antiferromagnetic correlation seems dominant. In this sense we call the present CeSi_x system as a ferromagnetic dense Kondo system whether it belongs to magnetic regime ($x < 1.83$) or nonmagnetic regime ($x > 1.83$). The values of the spin fluctuation temperature or the Kondo temperature, T_K , were evaluated from various physical quantities. For details, see ref. 8. An interesting finding was that thus obtained T_K varies smoothly with the Si concentration across the boundary between the nonmagnetic regime and the magnetic regime. However, with polycrystalline samples the confirmation of the Kondo effect by resistivity measurements was found to be almost impossible because of the existence of unavoidable microcracks in samples. Therefore it is very desirable to study the system with single crystals. The present paper describes our systematic study of single crystalline $\text{CeSi}_{1.86}$ (nonmagnetic regime) and $\text{CeSi}_{1.70}$ (magnetic regime).

§2. Experimental

Polycrystalline samples of $\text{CeSi}_{2.00}$ and $\text{CeSi}_{1.70}$ were prepared in an arc furnace under a pure Argon atmosphere. Ce of 99.9% purity and Si of 99.999% purity were used. These polycrystalline samples were casted into a rod-shape of 10 mm diameter. Then the floating-zone technique was employed to obtain single crystals of typical dimensions 8 mm in diameter and 30 mm in length. Because of the vapor pressure difference between Ce and Si the composition of the obtained single crystals may deviate from the starting polycrystalline samples. We tentatively assign the composition by comparing the values of the electronic specific heat coefficient γ of the single crystalline samples with those of the polycrystalline samples⁵⁾ (see §3.1). The specific heats were measured by the standard heat pulse method. The electrical resistivities were measured by a four terminal D.C. method. Spark cut samples were about $2 \times 2 \times 5 \text{ mm}^3$ in size. The magnetic susceptibility measurements were performed using a Faraday magnetometer with an applied magnetic field of 6 kOe.

§3. Results and Discussions

3.1 Specific heat

Results of the specific heat measurement of the single crystal grown from the $\text{CeSi}_{2.00}$ polycrystal are shown in Fig. 2(a). In the low temperature region below about 3 K, the specific heat can be expressed very well as

$$C = \gamma T, \quad (1)$$

with the γ value of

$$\gamma = 203 \text{ mJ/mole} \cdot \text{K}^2. \quad (2)$$

Comparing with the γ values of polycrystalline samples,⁵⁾ we notice that this γ value is much larger than that of $\text{CeSi}_{2.00}$ polycrystal. We consider that this discrepancy comes from the evaporation of Si during the process of the floating-zone single crystal growth. From the comparison with the value of polycrystalline samples,⁵⁾ we assign the composition of the single crystal as $\text{CeSi}_{1.86}$. So in the following we call this single crystal $\text{CeSi}_{1.86}$. We also show the specific heat data as C/T vs T plot in Fig. 2(b). The decrease of C/T with increasing temperature may be attributed to the spin fluctuation effect as discussed previously.⁵⁾ It is noted that this behavior is very similar to that observed in the polycrystalline $\text{CeSi}_{1.85}$.⁵⁾ This supports that our assignment of the composition is reasonable.

Next we show in Fig. 3(a) the specific heat of the single crystal grown from the $\text{CeSi}_{1.70}$ polycrystal. The data are also shown as a double logarithmic plot in Fig. 3(b). From this plot it is found that the low temperature specific heat far below the magnetic transition around 12 K shows a T -linear behavior. Such behavior was observed previously also for polycrystalline samples.⁵⁾ We tentatively take the coefficient of this T -linear term as γ in the magnetically ordered system. Thus obtained γ -value of the present single crystal is

$$\gamma = 78 \text{ mJ/mole} \cdot \text{K}^2. \quad (3)$$

This is very close to that of polycrystalline $\text{CeSi}_{1.70}$.⁵⁾ So the composition of the grown single crystal does not seem to deviate appreciably from the starting polycrystalline sample. In the following, we call this sample $\text{CeSi}_{1.70}$. However, we notice a big difference

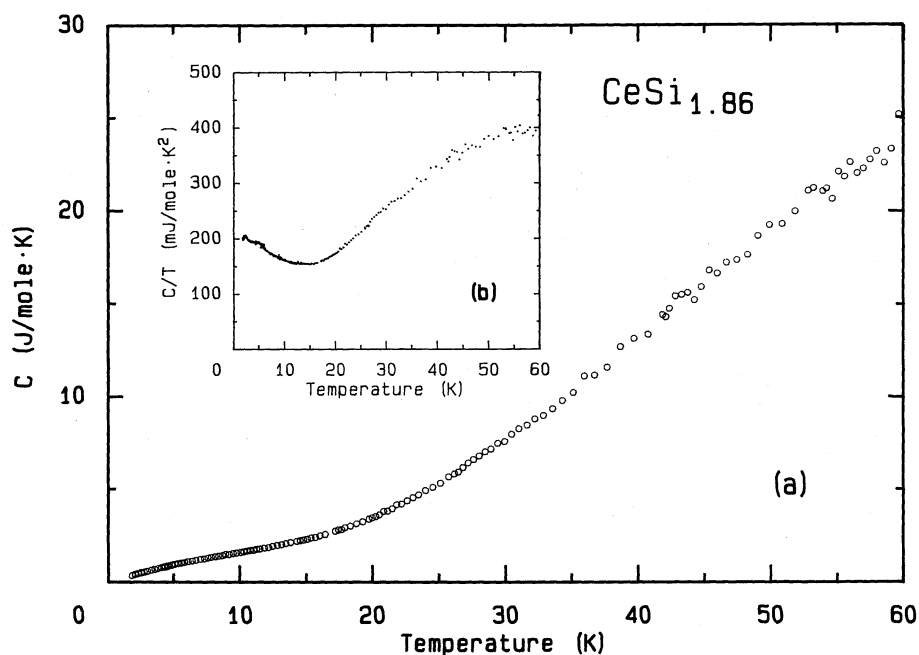


Fig. 2. (a) Specific heat of the single crystal obtained from polycrystalline $\text{CeSi}_{2.00}$. (b) C/T vs T plot of the specific heat of the single crystalline $\text{CeSi}_{1.86}$.

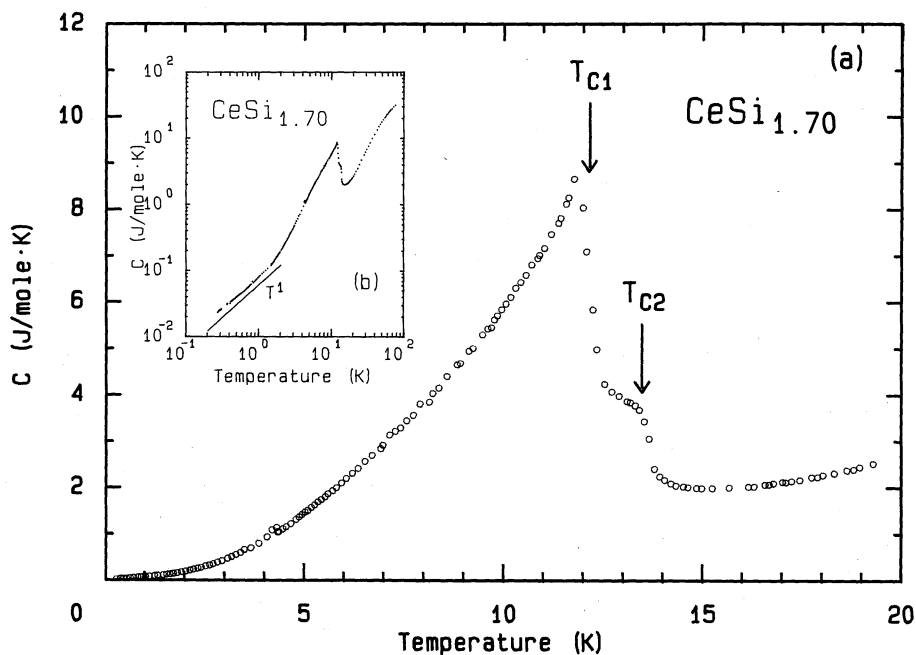


Fig. 3. (a) Specific heat of the single crystal obtained from polycrystalline $\text{CeSi}_{1.70}$. (b) Double logarithmic plot of specific heat of the single crystalline $\text{CeSi}_{1.70}$.

between the single crystal $\text{CeSi}_{1.70}$ and the previously studied polycrystal $\text{CeSi}_{1.70}$. That is, we observed two specific heat anomalies at 12.4 K (we call T_{c1}) and at 13.7 K (we call T_{c2}) in contrast with only one anomaly at 10.9 K in polycrystalline sample.²⁾ These two anomalies are related to the magnetic transitions.^{9,10)}

The magnetic entropy below T_{c2} may be evaluated from the specific heat data by subtracting the nonmagnetic contribution of the specific heat. We tentatively estimate the nonmagnetic contribution below T_{c2} by a smooth extrapolation of the measured specific heat curve above 25 K. The magnetic entropy below T_{c2} thus obtained is

$$S_m/R \ln 2 = 0.77. \quad (4)$$

3.2 Electrical resistivity

3.2.1 Electrical resistivity of $\text{CeSi}_{1.86}$ ¹¹⁾

The resistivity results of $\text{CeSi}_{1.86}$ are shown in Fig. 4(a). Both the resistivity along the a -axis, ρ_a and that along the c -axis, ρ_c , show a small temperature dependence around room temperature. At low temperatures, the behavior for the two directions shows a clear

contrast; ρ_c starts dropping suddenly around 50 K whereas ρ_a decreases more gradually. The low temperature parts of ρ_a and ρ_c are plotted against T^2 in Fig. 4(b). It is seen that below about 5 K both ρ_a and ρ_c can be expressed very well as

$$\rho_a(T) = 12.7[\mu\Omega \cdot \text{cm}] + 0.161[\mu\Omega \cdot \text{cm} \cdot \text{K}^{-2}]T^2, \quad (5)$$

$$\rho_c(T) = 28.5[\mu\Omega \cdot \text{cm}] + 1.13[\mu\Omega \cdot \text{cm} \cdot \text{K}^{-2}]T^2. \quad (6)$$

The magnetic contribution, ρ_m , may be obtained by subtracting the phonon contribution, ρ_{ph} from the measured resistivity. In order to assign ρ_{ph} the resistivity of polycrystalline LaSi_2 was also measured. To make single crystalline LaSi_2 was extremely difficult. The phonon contribution in LaSi_2 obtained by subtracting the residual resistivity from the measured one, was found to be fitted by the Bloch-Grüneisen formula with an assumed Debye temperature $\theta_D = 370$ K, which is in good agreement with 365 K obtained from the specific heat.¹²⁾

In Fig. 5 we plot the magnetic resistivities

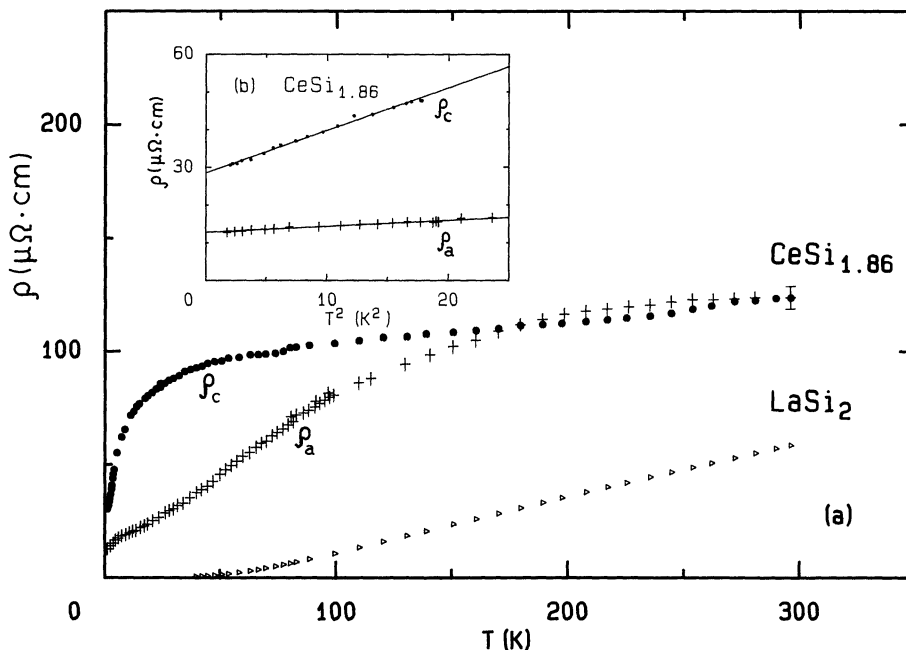


Fig. 4. (a) Plot of the total electrical resistivity of $\text{CeSi}_{1.86}$. (b) Electrical resistivity of $\text{CeSi}_{1.86}$ in the low temperature region, plotted as a function of T^2 .

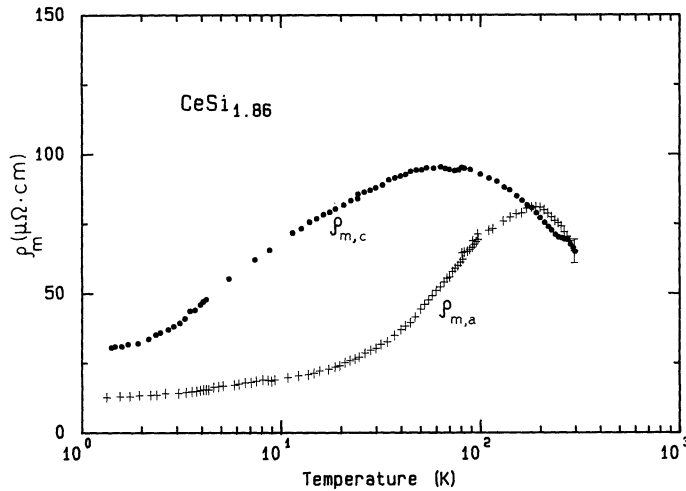


Fig. 5. Magnetic resistivity of $\text{CeSi}_{1.86}$ plotted against $\ln T$.

for the two direction $\rho_{m,a}$ and $\rho_{m,c}$, which show a clear maximum at around 200 K and 80 K, respectively. On the high temperature side of the respective maximum, $\rho_{m,c}$ almost follow a $\ln T$ dependence, while the temperature dependence of $\rho_{m,a}$ is less clear. A quantitative discussion is hampered by possible anisotropy in ρ_{ph} which is not taken into account here. However, if we note the small temperature dependence of ρ_a and ρ_c above about 200 K, we may safely conclude that both $\rho_{m,a}$ and $\rho_{m,c}$ decreases with increasing temperature around 300 K. These results clearly confirm the expectation made from the polycrystalline study that the CeSi_x system is a dense Kondo system. It is noted in Fig. 4(b) that the subtraction of ρ_{ph} does not influence the temperature dependence of ρ_a and ρ_c in the temperature region of the plot.

The decrease of $\rho_{m,a}$ and $\rho_{m,c}$ in the low temperature side of the respective maximum may be attributed to the development of the coherent Kondo state. The T^2 -dependence of the low temperature resistivity and the appearance of the coherent state clearly show that 4f-electrons of Ce atoms in $\text{CeSi}_{1.86}$ constitute a so-called Fermi liquid.

3.2.2 Electrical resistivity of $\text{CeSi}_{1.70}$

The resistivity results of $\text{CeSi}_{1.70}$ are shown in Fig. 6. Both ρ_a and ρ_c show only a small increase with decreasing temperature down to the magnetic transition temperature. The tem-

perature of the maximum are slightly different between ρ_a and ρ_c , that is, ρ_a has a maximum at around $T_{c1}=12.4$ K and ρ_c at around $T_{c2}=13.7$ K. On the low temperature side of the maximum, both ρ_a and ρ_c show only a slight decrease down to the lowest temperature investigated. So the extrapolated residual resistivities are very large as

$$\rho_{a,r}=128 [\mu\Omega \cdot \text{cm}], \quad (7)$$

$$\rho_{c,r}=155 [\mu\Omega \cdot \text{cm}]. \quad (8)$$

It seems very difficult to attribute these large residual resistivities to the static potential scattering due to the increase of the Si-deficiency in $\text{CeSi}_{1.70}$ compared with that in $\text{CeSi}_{1.86}$, as the order of magnitude of the amount of the Si-deficiency is almost same between them. It seems that if the amount of the Si-deficiency in CeSi_x exceeds some critical value, the development of the coherence is extremely suppressed even if the Ce-sublattice is not disturbed.

3.3 Magnetic susceptibility

3.3.1 Magnetic susceptibility of $\text{CeSi}_{1.86}$ ¹¹⁾

The susceptibility results of $\text{CeSi}_{1.86}$ are shown in Fig. 7(a), where χ_a and χ_c are the susceptibilities along the *a*- and *c*-axes, respectively. As expected from the tetragonal symmetry around the Ce ions, the susceptibility is anisotropic. At room temperature χ_c is larger than χ_a , and then the anisotropy reverses below 67 K. A Curie-Weiss fit is possible for χ_a

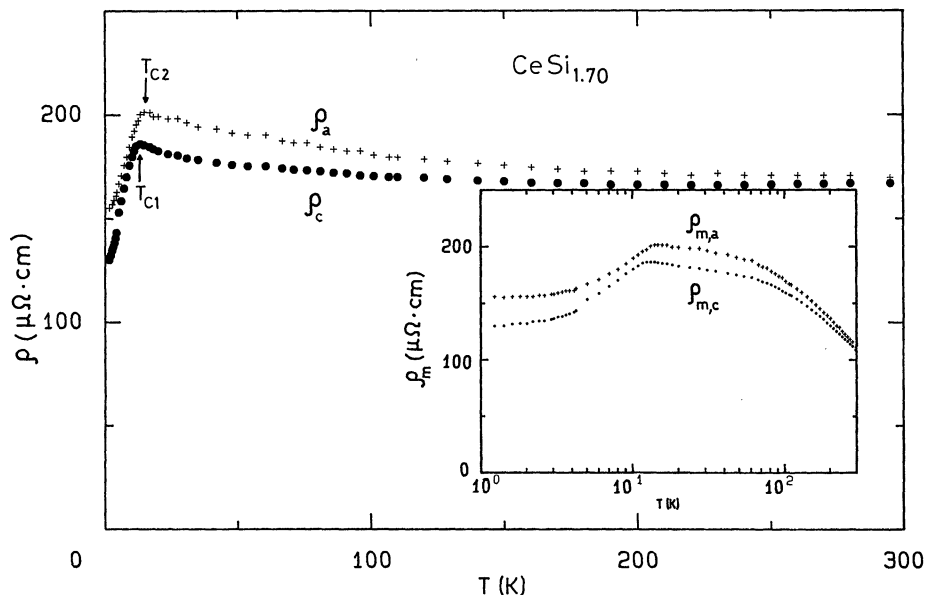


Fig. 6. (a) Plot of the total electrical resistivity of $\text{CeSi}_{1.70}$. (b) The temperature dependence of $\rho_{m,a}$ and $\rho_{m,c}$, where the phonon part is approximately subtracted by using the resistivity of LaSi_2 .

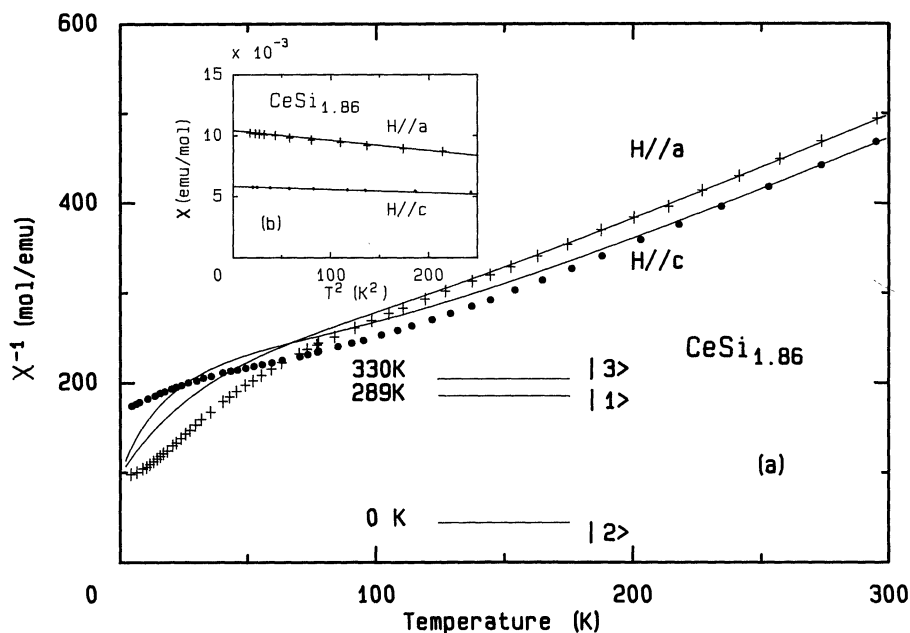


Fig. 7. (a) The reciprocal susceptibility of $\text{CeSi}_{1.86}$ plotted against temperature. Solid lines are the calculated values from the crystal field consideration, the level scheme of which is also shown in the figure. (b) Susceptibility of $\text{CeSi}_{1.86}$ in the low temperature region plotted against T^2 .

between 80 K and 300 K, and for χ_c over a somewhat narrower region from 150 K to 300 K. The values of paramagnetic Curie temperature θ thus obtained are

$$\theta_a = -137 \text{ K}, \quad (9)$$

$$\theta_c = -101 \text{ K}. \quad (10)$$

The values of effective moment μ_{eff} are

$$\mu_{\text{eff},a} = 2.65 \mu_B, \quad (11)$$

$$\mu_{\text{eff},c} = 2.60 \mu_B. \quad (12)$$

These are slightly larger than $2.53 \mu_B$ of free Ce^{3+} ion.

In Fig. 7(b), we also show the fit of our low temperature susceptibility with a T^2 -law

$$\chi(T) = \chi(0)(1 + AT^2). \quad (13)$$

Both χ_a and χ_c follow a T^2 -dependence over the region from 4.2 K to 15 K. The values of $\chi(0)$ and A are

$$\chi_a(0) = 1.04 \times 10^{-2} \text{ [emu/mole]}, \quad (14)$$

$$\chi_c(0) = 5.78 \times 10^{-3} \text{ [emu/mole]}, \quad (15)$$

$$A_a = -8.07 \times 10^{-4} \text{ [K}^{-2}\text{]}, \quad (16)$$

$$A_c = -4.50 \times 10^{-4} \text{ [K}^{-2}\text{]}. \quad (17)$$

3.3.2 Magnetic susceptibility of $\text{CeSi}_{1.70}$

The susceptibility results of $\text{CeSi}_{1.70}$ are shown in Fig. 8. They diverge at around T_c . Comparing this result with Fig. 7(a), it is seen that the anisotropic behavior is almost same as $\text{CeSi}_{1.86}$. This makes a contrast with the resistivity results in which the anisotropic behavior is smeared out in $\text{CeSi}_{1.70}$ compared with $\text{CeSi}_{1.86}$. These results suggest that the anisotropic aspect of the magnetic susceptibility comes from a single ion character. Therefore it is worthwhile to see whether or not the observed anisotropic behavior of the susceptibility can be explained with the crystal field effect.

3.3.3 Crystal field considerations

The multiplet $J=5/2$ of Ce^{3+} ion splits into three doublets in the tetragonal crystal field, the Hamiltonian of which is expressed as

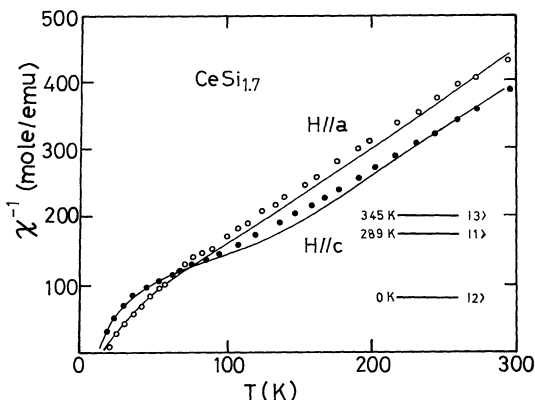


Fig. 8. The reciprocal susceptibility of $\text{CeSi}_{1.70}$ plotted against temperature. Solid lines are the calculated values from the crystal field consideration, the level scheme of which is also shown in the figure.

$$H_{\text{cr}} = B_2^0 O_2^0 + B_4^0 O_4^0 + B_4^4 O_4^4, \quad (18)$$

where c -axis is taken as z -axis and

$$O_2^0 = 3J_z^2 - J(J+1), \quad (19)$$

$$O_4^0 = 35J_z^4 - 30J(J+1)J_z^2 + 25J_z^2 - 6J(J+1) + 3J^2(J+1)^2, \quad (20)$$

$$O_4^4 = (J_+^4 + J_-^4)/2. \quad (21)$$

The eigen function of the three doublets are expressed as

$$|1\pm\rangle = \cos\theta |\pm 5/2\rangle + \sin\theta |\mp 3/2\rangle, \quad (22)$$

$$|2\pm\rangle = \sin\theta |\pm 5/2\rangle - \cos\theta |\mp 3/2\rangle, \quad (23)$$

$$|3\pm\rangle = |\pm 1/2\rangle, \quad (24)$$

where θ takes a value in the region $0 \leq \theta \leq \pi/2$. The energy eigen value of each state and θ are expressed with B_2^0 , B_4^0 and B_4^4 as

$$E_1 = \langle 1\pm | H_{\text{cr}} | 1\pm \rangle, \quad (25)$$

$$E_2 = \langle 2\pm | H_{\text{cr}} | 2\pm \rangle, \quad (26)$$

$$E_3 = \langle 3\pm | H_{\text{cr}} | 3\pm \rangle, \quad (27)$$

$$\theta = \cos^{-1} \frac{\text{sgn}(B_4^4)(B_2^0 + 20B_4^0) + \sqrt{(B_2^0 + 20B_4^0)^2 + 20(B_4^4)^2}}{2\sqrt{(B_2^0 + 20B_4^0)^2 + 20(B_4^4)^2}}, \quad (28)$$

where

$$\text{sgn}(B_4^4) = \begin{cases} 1; & B_4^4 \geq 0 \\ -1; & B_4^4 < 0 \end{cases}. \quad (29)$$

Magnetic susceptibility is obtained with the relation

$$\chi_v = \frac{N_A (g_J \mu_B)^2}{k_B Z} \sum_{m,n} \frac{e^{-E_m/T} - e^{-E_n/T}}{E_n - E_m} |\langle m | J_v | n \rangle|^2, \quad (30)$$

where

$$Z = 2 \sum_m e^{-E_m/T}, \quad (31)$$

and v expresses a direction of the crystal axis (a or c -axis), N_A is the Avogadro's number, k_B is the Boltzman constant and g_J is Lande's g -factor.

Using eqs. (25)–(27) in eq. (30), we obtain

$$\chi_{\text{cr},a}(T) = \frac{2N_A (g_J \mu_B)^2}{k_B Z} \left[5 \sin^2 2\theta \frac{e^{-E_1/T} + e^{-E_2/T}}{4T} + \frac{9e^{-E_3/T}}{4T} + 5 \cos^2 2\theta \frac{e^{-E_1/T} - e^{-E_2/T}}{2(E_2 - E_1)} \right. \\ \left. + 4 \sin^2 \theta \frac{e^{-E_1/T} - e^{-E_3/T}}{E_3 - E_1} + 4 \cos^2 \theta \frac{e^{-E_2/T} - e^{-E_3/T}}{E_3 - E_2} \right], \quad (32)$$

$$\chi_{\text{cr},c}(T) = \frac{2N_A (g_J \mu_B)^2}{k_B Z} \left[(1 + 4 \cos 2\theta)^2 \frac{e^{-E_1/T}}{4T} + (1 - 4 \cos 2\theta)^2 \frac{e^{-E_2/T}}{4T} \right. \\ \left. + \frac{e^{-E_3/T}}{4T} + 2(2 \sin 2\theta)^2 \frac{e^{-E_1/T} - e^{-E_2/T}}{E_2 - E_1} \right]. \quad (33)$$

In order to proceed the calculation, the crystal field Hamiltonian eq. (18) is written in the form

$$H_{\text{cr}} = W[(1 - |Y|)O_2^0 + (1 - |X|)YO_4^0 + XYO_4^4], \quad (34)$$

where

$$|X|, |Y| \leq 1. \quad (35)$$

With eqs. (25)–(28) and (32)–(34), it is seen that for fixed values of W and Y , the susceptibility does not depend on the sign of X . The crystal field Hamiltonian for the cubic symmetry is expressed as

$$H_{\text{cr}} = B_4(O_4^0 + 5O_4^4). \quad (36)$$

Therefore, in order to include the cubic symmetry case, the following calculation is performed with positive sign of X . Here, the parameter W represents the energy scale. At first the calculation is made with the following condition

(i) $\chi_{\text{cr},a}(T = \Delta_1/10) > \chi_{\text{cr},c}(T = \Delta_1/10)$, $\chi_{\text{cr},a}(T = 10\Delta_2) < \chi_{\text{cr},c}(T = 10\Delta_2)$, where Δ_1 and Δ_2 are the energy differences between the ground state and the first excited state and between the ground state and the second excited state, respectively ($\Delta_2 > \Delta_1 > 0$). Next, we take into account the second condition

(ii) $\chi_{\text{cr},a}(T = T_0) = \chi_{\text{cr},c}(T = T_0)$, where T_0 is

the temperature at which the measured susceptibility along a - and c -axes coincide with each other, that is $T_0 = 67$ K for $\text{CeSi}_{1.86}$ and $T_0 = 65$ K for $\text{CeSi}_{1.70}$. The parameter W is varied to satisfy this condition and then the third condition

(iii) $[\chi_{\text{cr},a}^{-1} - \chi_{\text{cr},c}^{-1}]_{\text{cal}} = [\chi_{\text{cr},a}^{-1} - \chi_{\text{cr},c}^{-1}]_{\text{obs}}$ at room temperature is used to select the most desirable combinations of W , X and Y . Examples of the susceptibility calculated with thus selected parameters are shown in Fig. 9. Finally, we must take into account the exchange and the Kondo effects.

For $\text{CeSi}_{1.70}$, this is made by assuming that these effects only slide the calculated crystal field susceptibility as a whole. Although this procedure assumes that the effects are isotropic, calculated susceptibility fits the experimental data well as shown in Fig. 8. The finally selected parameters are

$$B_2^0 = -3.823 \text{ K}, B_4^0 = 0.859 \text{ K}, B_4^4 = 4.477 \text{ K}, \\ \cos \theta = 0.882, \sin \theta = 0.472, \quad (37) \\ E_1 = 289 \text{ K}, E_2 = 0 \text{ K}, E_3 = 345 \text{ K}.$$

For $\text{CeSi}_{1.86}$ the low temperature susceptibility remains at a finite value because of the Kondo effect. So the above mentioned simple procedure is useless. In this case we must take into account the Kondo effect more seriously.

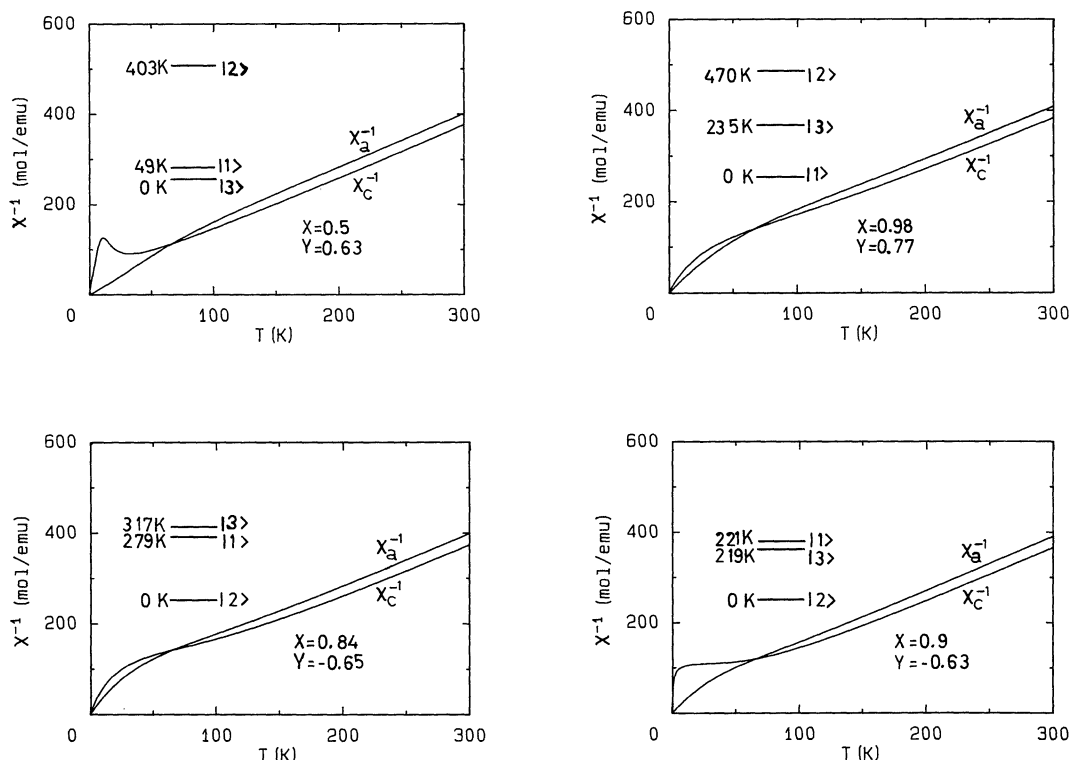


Fig. 9. Calculated susceptibility χ^{-1} with the most desirable combinations of W , X and Y which satisfy the conditions (i)~(iii) (see the text).

As the first approximation we put the fourth condition

(iv) $[\chi_a(0)/\chi_c(0)] = [(g_{\text{eff},a}/g_{\text{eff},c})^2]_{\text{cal}}$, where g_{eff} is the effective g value of the ground doublet. Then we obtain the final selection of the parameters as

$$\begin{aligned} B_2^0 &= -2.755 \text{ K}, \quad B_4^0 = 0.846 \text{ K}, \quad B_4^4 = 4.36 \text{ K}, \\ \cos \theta &= 0.891, \quad \sin \theta = 0.454, \\ E_1 &= 289 \text{ K}, \quad E_2 = 0 \text{ K}, \quad E_3 = 330 \text{ K}. \end{aligned} \quad (38)$$

The comparison between the measured and the calculated susceptibilities is shown in Fig. 7(a).

It is noted that according to the present fitting procedure, the ground state is, $|2\pm\rangle$ both for $\text{CeSi}_{1.86}$ and $\text{CeSi}_{1.70}$. Further the finally selected parameter θ is very close to the value for the cubic crystal field case.

$$\cos \theta = 0.913, \quad \sin \theta = 0.408. \quad (39)$$

So the ground state, $|2\pm\rangle$ is considered nearly as Γ_7 .

3.4 Kondo temperature

Until now, there has been no theoretical expression for the Kondo temperature of a dense Kondo system. However, it is widely accepted that the Kondo temperature expression for the single impurity Kondo problem may give an appropriate characteristic temperature of the dense system. The Kondo temperatures given in ref. 8 were obtained with such a way. Since that time, there has been a big theoretical progress to solve exactly the single impurity Kondo problem.^{13,14)}

Recently, Kawakami and Okiji have derived¹⁵⁾ the exact solution of the Anderson model including crystalline field of cubic symmetry. If we consider only the ground doublet, their argument may be extended in the case of tetragonal crystal field as

$$\gamma = \frac{\pi}{6T_c}, \quad (40)$$

and

$$\chi(0) = \frac{N_A (g_{\text{eff}} \mu_B)^2}{4\pi k_B T_e}. \quad (41)$$

It is noted that the Kondo temperature T_e given here is taken as an effective Kondo temperature in the low temperature region. With eqs.(40) and (41), we obtain the Kondo temperatures for $\text{CeSi}_{1.86}$ as

$$T_e[\gamma]_{1.86} = 21.1 \text{ K}, \quad (42)$$

and

$$T_e[\chi(0)]_{1.86} = 6.8 \text{ K}. \quad (43)$$

There is rather large difference between $T_e[\gamma]$ and $T_e[\chi(0)]$. Such a discrepancy was already noted in the polycrystalline study.⁸⁾ This discrepancy may be due to the fact that the system is close to a ferromagnetic instability. That is, the large finite value of $\chi(0)$ comes not only from the Kondo effect but also from the enhancement due to the magnetic interaction among Ce ions. Although such a magnetic interaction also enhances the electronic specific heat coefficient γ , as a paramagnon effect, the effect is much weaker as logarithmic compared with the enhancement of the susceptibility. Another point to be noted is that we did not take into account the Van Vleck contribution to the extrapolated experimental value of $\chi(0)$. Such a consideration will make the discrepancy smaller. Therefore, here we take $T_e[\gamma]$ as the effective Kondo temperature of $\text{CeSi}_{1.86}$.

For the magnetically ordered $\text{CeSi}_{1.70}$ the most reliable estimation of the effective Kondo temperature for the ground doublet may be from the magnetic entropy below the magnetic transition temperature. That is, the reduction of the magnetic entropy compared with $R \ln 2$ is considered due to the Kondo effect which already exists above the magnetic transition temperature. Using the numerically calculated entropy value by Desgranges and Schotte,¹⁶⁾ we obtain the effective Kondo temperature of $\text{CeSi}_{1.70}$ as

$$T_e[S]_{1.70} = 4.8 \text{ K}. \quad (44)$$

§8. Concluding Remarks

We have made single crystals of CeSi_x . Comparing the results of specific heat measurements with the polycrystalline data, we assigned their composition as $\text{CeSi}_{1.86}$

(nonmagnetic regime) and $\text{CeSi}_{1.70}$ (magnetic regime).

Electrical resistivity measurements on $\text{CeSi}_{1.86}$ clearly show the typical Kondo behavior, which unambiguously tells that CeSi_x system is a ferromagnetic dense Kondo system. Although the resistivities at low temperatures show a clear coherence phenomena in $\text{CeSi}_{1.86}$, the residual resistivity of $\text{CeSi}_{1.70}$ is very large, which we attribute to the destruction of the coherence. Further the large anisotropic behavior of the resistivity observed for $\text{CeSi}_{1.86}$ almost disappears in $\text{CeSi}_{1.70}$.

In contrast with the electrical resistivity data, the anisotropic behavior of magnetic susceptibility does not show appreciable difference between $\text{CeSi}_{1.86}$ and $\text{CeSi}_{1.70}$. This motivated us to analyze the anisotropic aspect of magnetic susceptibility within the framework of the simple crystalline field theory. According to the analysis the most probable ground state is, $|2\pm\rangle$ both in $\text{CeSi}_{1.86}$ and in $\text{CeSi}_{1.70}$. The wave functions do not deviate so much from the Γ_7 doublet in the cubic crystalline field case.

Finally, it is important to note that the single crystalline $\text{CeSi}_{1.70}$ shows two successive transitions at T_{c1} and T_{c2} . This is a big contrast with the polycrystalline data.²⁾ In the following paper,¹⁰⁾ we will discuss the magnetic states of this single crystalline $\text{CeSi}_{1.70}$.

Acknowledgments

It is a pleasure to acknowledge useful discussions with T. Kasuya, M. Tachiki, S. Maekawa, Y. Kuramoto, N. Kawakami and A. Okiji.

References

- 1) H. Yashima, T. Satoh, H. Mori, D. Watanabe and T. Ohtsuka: *Solid State Commun.* **41** (1982) 1.
- 2) H. Yashima and T. Satoh: *Solid State Commun.* **41** (1982) 723.
- 3) H. Yashima, Chui Feng Lin, T. Satoh, H. Hiroyoshi and K. Kohn: *Solid State Commun.* **57** (1986) 793.
- 4) H. Yashima, T. Satoh and H. Hiroyoshi: *High Field Magnetism*, ed. M. Date (North-Holland, Amsterdam, 1983) p. 191.
- 5) H. Yashima, N. Sato, H. Mori and T. Satoh: *Solid State Commun.* **43** (1982) 595.
- 6) W. F. Brinkman and S. Engelsberg: *Phys. Rev.* **169** (1968) 417.

- 7) K. Makoshi and T. Moriya: J. Phys. Soc. Jpn. **35** (1975) 10.
 - 8) H. Yashima, H. Mori, T. Satoh and K. Kohn: Solid State Commun. **43** (1982) 193.
 - 9) N. Sato, M. Kohgi, T. Satoh, Y. Ishikawa, H. Hiroyoshi and H. Takei: J. Magn. & Magn. Mater. **52** (1985) 360.
 - 10) N. Sato, M. Kohgi, H. Hiroyoshi, K. Torizuka, A. Sawada and T. Satoh: in preparation for publication.
 - 11) N. Sato, H. Mori, H. Yashima, T. Satoh and H. Takei: Solid State Commun. **51** (1984) 139.
 - 12) T. Satoh and T. Ohtsuka: Phys. Lett. **20** (1966) 565.
 - 13) N. Andrei, K. Furuya and J. H. Lowenstein: Rev. Mod. Phys. **55** (1983) 331.
 - 14) A. M. Tsveleck and P. B. Wiegmann: Adv. Phys. **32** (1983) 453.
 - 15) N. Kawakami and A. Okiji: *Proc. 8th Taniguchi Symposium, 1985*, ed. T. Kasuya and T. Saso (Springer-Verlag) p. 57
 - 16) H. U. Desgranges and K. D. Schotte: Phys. Lett. **A91** (1982) 240.
-